Atmospheric Environment 42 (2008) 7215–7233

Contents lists available at ScienceDirect

Atmospheric Environment

journal homepage: www.elsevier.com/locate/atmosenv

Development of a high-resolution (1 km × 1 km, 1 h) emission model for Spain: The High-Elective Resolution Modelling Emission System (HERMES)

José María Baldasano [a,b,*], Leonor Patricia Güereca [a], Eugeni López [a], Santiago Gassó [a,b], Pedro Jimenez-Guerrero [a]

[a] Earth Sciences Department, Barcelona Supercomputing Center-Centro Nacional de Supercomputación (BSC-CNS), Barcelona, Spain
[b] Project Engineering Department, Technical University of Catalonia (UPC), Barcelona, Spain

ARTICLE INFO

Article history:
Received 7 March 2008
Received in revised form 8 July 2008
Accepted 14 July 2008

Keywords:
Emission inventories
Anthropogenic emissions
Biogenic emissions
Models
High-resolution modelling

ABSTRACT

This work presents the results of the development and application of the High-Elective Resolution Modelling Emission System (HERMES). HERMES generates the emissions for Spain needed for the application of high-resolution chemistry transport models, taking the year 2004 as reference with a temporal resolution of 1 h and a spatial resolution of 1 km^2 considering both anthropogenic (power generation, industrial activities, on-road traffic, ports, airports, solvent use, domestic and commercial fossil fuel use) and biogenic sources (vegetation), using a bottom–up approach, up-to-date information and state-of-the-art methodologies for emission estimation. HERMES is capable of calculating emissions by sector-specific sources or by individual installations and stacks. The annual addition of hourly sectorial emissions leads to an estimation of total annual emissions as follows: NO_x, 795 kt; NMVOCs, 1025 kt; CO, 1236 kt; SO_2, 1142 kt and TSP, 180 kt; which are distributed principally in the greater areas of the main cities, highways and large point sources. NO_x, SO_2 and $PM_{2.5}$ highly correlate with the power generation by coal use, achieving higher emission levels during summertime due to the increase of electricity demand by cooling systems. NMVOCs show high correlation with temperature and solar radiation (mainly as a consequence of the important weight of biogenic emissions) causing the maximum emissions during the daylight hours of summer months. CO emissions are mostly influenced by the on-road traffic; consequently the higher emissions are attained in summer because of the increase of daily average traffic during holidays. The most significant total emission sources are on-road traffic (38%), combustion in power generation plants (33%), biogenic sources (12%) and combustion in manufacturing industries (9%). The inventory generated with HERMES emission model has been successfully integrated within the Spanish Ministry of the Environment's air quality forecasting system (Caliope project), being the emission core for the validation and assessment of air quality simulations in Spain.

1. Introduction

Emissions models are mathematical representations of the pollutants emitted directly from sources and constitute an essential tool for policy, regulatory and scientific purposes in topics related to air quality (Parra et al., 2006;

* Corresponding author. Project Engineering Department, Technical University of Catalonia (UPC), Jordi Girona 29, Edificio Nexus II, 08034 Barcelona, Spain.
E-mail address: jose.baldasano@bsc.es (J.M. Baldasano).

1352-2310/$ – see front matter © 2008 Elsevier Ltd. All rights reserved.
doi:10.1016/j.atmosenv.2008.07.026

Jiménez-Guerrero et al., 2008) and climate change (Unger et al., 2008) due to a direct relationship between the air pollutants and the environmental problems, which also represent an important health risk (Carnevale et al., 2006; Saamali et al., 2007). For this reason, the amount calculation of pollutants released in a given area during a certain period of time is the basic tool for decision makers to identify highly polluted areas and take action to reduce emissions (Economopoulos, 1993; Baldasano, 1998).

Up-to-date, most emission models are characterised by annual calculation periods, are referred to a territory limited by national administrative borders and require the use of predefined methodologies. This approach is usually based on aggregated-statistical methodologies (top–down approach) (Tuia et al., 2007). In the case of Europe, the EMEP/CORINAIR estimates emissions for a pan-European domain with a spatial resolution of 50 km × 50 km on an annual basis (Vestreng et al., 2005), according to 11 source categories. However, for high-resolution air quality modelling purposes, there are recognised limitations in the EMEP inventories and their spatial and temporal resolution needs to be improved.

During the last years the scientific knowledge and the feasible access to the information have significantly increased, allowing the use of better emission models and quality emission factors, comprising more activities and information data. Thus, when developing emission models for high-resolution air quality management or modelling, a high spatial, temporal and chemical disaggregation is required in order to accurately characterise the variety of emission sources (bottom–up approach) (Colvile et al., 2001; Kannari et al., 2007).

Currently, there is a remarkable tendency in the different states towards the development of high-resolution emission models (1 km^2) following bottom–up approaches. For example, in Europe the United Kingdom has developed the National Atmospheric Emissions Inventory (NAEI, 2007) taking the year 2005 as reference. EMICAT (Parra et al., 2006) estimates the primary air pollutants for Catalonia (Spain) for the year 2000; and ESCOMPTE program (Cros et al., 2004; François et al., 2005) estimates emissions over the Marseille area in southeastern France for the year 1999 (annual values) and for the summers of 2000 and 2001 (hourly values). Outside Europe, Kannari et al. (2007) estimate an inventory with hourly and 1 km^2 resolution for the year 2000 in Japan. Several efforts have been also carried out to estimate emissions on scales covering counties, departments or municipalities (e.g. Streets et al., 2003; Chang et al., 2007; Monteiro et al., 2007; USEPA, 2008; among others). All this information is comprised in Table 1.

In the particular case of Spain, its complex topographic conditions, land use variation, the influence of a great number of climatic variables (surface and soil temperature, humidity, etc.) and the complex pattern of both natural and anthropogenic emissions are driving forces mechanisms on air pollutants dispersion and transformation (Jiménez et al., 2006). Therefore the development and use of specifically-developed emission models that take into account these particularities with very high spatial and temporal resolution (1 km^2 and 1 h) is necessary.

Under this framework, the BSC-CNS has developed the High-Elective Resolution Modelling Emissions System (HERMES) to generate the emission inventory in Spain, taking the year 2004 as the reference period. HERMES compiles the progress on emission modelling of the Environmental Modelling Laboratory of the Technical University of Catalonia (UPC) (Costa and Baldasano, 1996; Gomez and Baldasano, 1999; Delgado et al., 2000; Arévalo et al., 2004; Parra et al., 2004, 2006; among others). HERMES estimates the atmospheric emissions with a temporal resolution of 1 h and a spatial resolution of 1 km^2 and generates results according to the European Environmental Agency's Selected Nomenclature for Air Pollution (SNAP), which is the official activity classification system applied by the European Commission in the CORINAIR emission inventory. Furthermore, HERMES has the capacity of presenting results according to individual installation, industrial activities, land use classification or type of pollutants or process (fugitive, evaporative, hot or cold emissions).

Some of the characteristics of HERMES are: (1) use of up-to-date information; (2) use of emission estimation methodologies compiling the state-of-the-art in different sectors and activities; (3) definition of the emission patterns coming from primary gaseous and particulate pollutants (including precursors of tropospheric ozone and secondary aerosols) together with greenhouse gases emissions; (4) selective chemical speciation of emissions. The chemical mechanisms currently included in HERMES are the Carbon Bond-IV (Gery et al., 1989) and MELCHIOR2 (Derognat et al., 2003); (5) capability of generation of graphic and alphanumeric information with very high-resolution; (6) development of the model following a quality protocol that guarantees the reliability of the results; (7) implementation of the emission methodologies for their easy revision and actualisation; and (8) combination of emissions from different sources to perform sensibility analysis or to study the sectorial contribution of each source to the emissions.

This work describes the detailed methodologies and approaches of HERMES, together with a deep discussion of the results for the emission inventory of Spain for the year 2004. HERMES is capable of estimating the emissions for Spain with a spatial resolution of 1 km × 1 km and temporal resolution of 1 h for chemistry transport modelling applications. Furthermore, the model constitutes the emission core of the operational air quality forecasting system for Spain developed under the Caliope project funded by the Spanish Ministry of the Environment (http://www.bsc.es/caliope), whose operational domain corresponds to Europe (5736 km × 4776 km), the Iberian Peninsula–Balearic Islands (1596 km × 1596 km) and Barcelona–Madrid Greater Areas (146 km × 146 km) with a spatial resolution of 12 km, 4 km and 1 km, respectively (Fig. 1). Hence, the results and discussion presented in this work for HERMES emissions are referred to the operational domain set for Spain in order to validate the Caliope air quality simulations (Baldasano et al., 2007; Jiménez-Guerrero et al., 2007).

HERMES has been implemented in a high-performance parallel machine such as the MareNostrum supercomputer hold by the BSC-CNS where the Caliope system is

Table 1
Summary of emission inventories

Emission inventories	Sources	Emission sources	Compounds included	Temporal resolution	Spatial resolution	Use
GLOBAL SCALE						
EDGAR 32FT2000	van Aardenne et al., 2005	Anthropogenic	NO_x, NMVOC, CO, SO_2, CO_2, CH_4, N_2O, CFCs, HFCs, PFCs, SF_6	Annual, 2000	Global, 1° × 1° (approx 10,000 km^2)	Regulatory, scientific
GEIA	GEIA/ACCENT, 2005	Anthropogenic and natural	NO_x, NMVOC, CO, SO_2, NH_3, CO_2, CH_4, N_2O, HFCs, PFCs, MFC, Pb, Hg	Annual, seasonal, and monthly, 1990	Global, 1° × 1° (approx 10,000 km^2)	Regulatory, scientific
UNFCCC	UNFCCC, 2008	Anthropogenic	CO_2, CH_4, N_2O, HFCs, PFCs, SF_6, NO_x, NMVOC, CO, SO_2	Annual, 1990–2005	Tabulated for the involved countries	Regulatory
POET	Granier et al., 2005	Anthropogenic and natural	CO, NO_x, C_2H_4, C_2H_6, C_3H_6, C_3H_8, CH_3OH, Acetona, Isoprenos, Terpenos	Annual and monthly, 1990–2000	Global, 1° × 1°	Regulatory, scientific
RETRO	Schultz et al., 2007	Anthropogenic	CO, NO_x, alcohols, C_2H_4, C_2H_6, C_3H_6, C_3H_8, butanes, pentanes, hexanes, methanol, other alkanes, acids, chlorinated hydrocarbons, ethers, esters, ethyne, toluene, benzene, xylene, other aromatics, ketones, other VOC, trimethylbenzene, N_2O, NH_3, BC, OT, TC, $PM_{2.5}$, TPM	Monthly, 1960–2000	Global, 0.5° × 0.5°	Regulatory, scientific
GFED v.2	van der Werf et al., 2006	Biomass burning	CO_2, CH_4, C, CO, NO_x, N_2O, H_2, BC, OC, $PM_{2.5}$, TPC, TC	Monthly, 1997–2006	Global, 1° × 1°	Scientific
REGIONAL SCALE						
EMEP/CORINAIR	EEA, 2007	Anthropogenic and natural	NO_x, NMVOC, CO, SO_2, NH_3, 9 heavy metals, 10 POPs, $PM_{2.5}$, PM_{10}, TSP	Annual, Official European inventories 1980–2005	Europe, 50 km × 50 km (2500 km^2)	Regulatory, scientific
TNO/CEPMEIP	CEPMEIP, 2008	Anthropogenic	$PM_{2.5}$, PM_{10}, TSP	Annual, 1995	Europe, 50 km × 50 km (2500 km^2)	Regulatory
GENEMIS/ EUROTRAC2	Friedrich and Reis, 2004	Anthropogenic and biogenic	NO_x, NMVOC, CO, SO_2, NH_3, $PM_{2.5}$, PM_{10}, TSP	Annual, 1998	Europe, 50 km × 50 km (2500 km^2)	Scientific
EPER	Pulles et al., 2007	Industrial emissions	NO_x, NMVOC, CO, SO_2, NH_3, PM_{10}, CO_2, CH_4, N_2O, PFC, HFC, SF_6	Annual, 2001	Europe, by country and geographical coordinates	Regulatory
ABBI Asia	Michel et al., 2005	Biomass burning	CO, NO_2, NO, CO_2, CH_4, SO_2, ethane, ethene, propane, propene, butanes, butenes, methanol, ethanol, formaldehyde, aldehydes, acetone, ketones, etc.	Daily, March–May 2000 and March–May 2001	Asia, 1° × 1°	Scientific
REAS Asia	Ohara et al., 2007	Anthropogenic	CO, NO_x, CO_2,	Annual, 1980–2020	Asia, 0.5° × 0.5°	Regulatory, scientific
REGIONAL TO LOCAL SCALE						
NEI	USEPA, 2008	Anthropogenic	NO_x, COV, CO, SO_2, NH_3, $PM_{2.5}$, PM_{10}	Annual, 2002	United States, by county	Regulatory, scientific
NAEI	Dore et al., 2007	Anthropogenic and natural	NO_x, NMVOC, CO, SO_x, NH_3, PM_{10}, CO_2, CH_4, N_2O	Hourly, 2005	United Kingdom, 1 km^2 × 1 km^2	Regulatory, Scientific
CITEPA	Chang et al., 2007	Anthropogenic and natural	COV, NO_x, CO	Annual, 2005	France	Regulatory, scientific
EAGrid2000	Kannari et al., 2007	Anthropogenic and natural	SO_2, NO_x, NMVOC, NH_3, CO, PM_{10}	Hourly by month, from April 2000–to March 2001	Japan	Scientific

(*continued on next page*)

Table 1 (*continued*)

Emission inventories	Sources	Emission sources	Compounds included	Temporal resolution	Spatial resolution	Use
BSC (EMICAT-EMIVAL)	Parra et al., 2006; Arévalo et al., 2004	Anthropogenic and natural	NO_x, NMVOC, CO, SO_2, NH_3, $PM_{2.5}$, PM_{10}, TSP	Hourly, 2000	North–eastern Iberian Peninsula, $1\ km^2 \times 1\ km^2$	Scientific
ESCOMPTE	François et al., 2005	Anthropogenic and natural	NO_x, NMVOC, CO, SO_2, NH_3, CO_2	Annual, 1999. Hourly, summer 2000 and 2001	Southeast of France (Marsella), $1\ km^2 \times 1\ km^2$	Scientific
BSC-HERMES	This work	Anthropogenic and natural	NO_x, NMVOC, CO, SO_2, NH_3, $PM_{2.5}$, PM_{10}, TSP, nitrate, sulphate, ammonia, BC, EC, OC	Hourly, base year 2004 (updateable)	Iberian Peninsula, Balearic and Canary Islands, $1\ km^2 \times 1\ km^2$	Scientific

integrated. The computational implementation of HERMES consists of two well-differentiated parts: (1) calculation; and (2) data management (both input and output). The calculation part is fully developed in C programming language and is run under a supercomputing framework. The pre-processing of data and cartography edition, as well as the management of operational data and analysis of results is performed through ESRI ArcGIS 9.2 Geographic Information System (GIS).

2. Methodology

The general framework of HERMES is illustrated in Fig. 2 where the base information, emission computation and output information are showed. HERMES considers the emissions from the following sources: (1) power generation plants; (2) industrial installations (plus waste incineration, which follows the same calculation methodology); (3) domestic and commercial fossil fuel use; (4) domestic and commercial solvents use; (5) road transport; (6) ports; (7) airports; and (8) biogenic emissions. The model uses a bottom–up approach except for domestic and commercial fossil fuel use, where a top–down approach was adopted and regional emissions were allocated to fine grid cells by surrogate indexes.

HERMES considers as primary air pollutants nitrogen oxide (NO_x), non-methane volatile organic compounds (NMVOC), carbon monoxide (CO), sulphur dioxide (SO_2), total suspended particles (TSP) and particulate mater (PM_{10} and $PM_{2.5}$). For power generation, industrial sources, use of fossil fuels by residential and commercial sectors and road transport the following greenhouse gases (GHG) have been estimated: carbon dioxide (CO_2), methane (CH_4) and nitrous oxide (N_2O).

The domain of HERMES covers the entire Spain, dividing the territory in squared cells of 1 km^2. The temporal resolution is 1 h and the baseline data correspond to the year 2004.

All this methods and steps have been implemented under a QA/QC protocol. In this sense, a qualitative evaluation of the uncertainty through the Data Attribute Rating System (DARS) (USEPA, 2003) as adapted by Parra (2004) has been carried out in Table 2, which also summarises the origin of the information used in the estimation of emissions for each of the aforementioned sectors. DARS classifies in a scale ranging from 1 (worst estimation) to 10 (best estimation) different attributes of the emission factors and the parameters used as base information to determine the activity. The attributes analysed are: (1) measurement method, referring to the qualification of the emission factors or base parameters, according to the measurement method used for their estimation; (2) spatial congruency, which establishes the representation of the emission factor or the activity parameter to the case of Spain; and (3) temporal congruency, qualifying the representation of the emission factor or the activity parameter throughout the year. For each attribute, the average of the qualification of the base activity parameters is obtained multiplied by the corresponding qualification for the emission factors. Finally, to quantify the quality of the emissions, the average is obtained for the multiplication of the three attributes analysed. This system identifies the aspects related to the

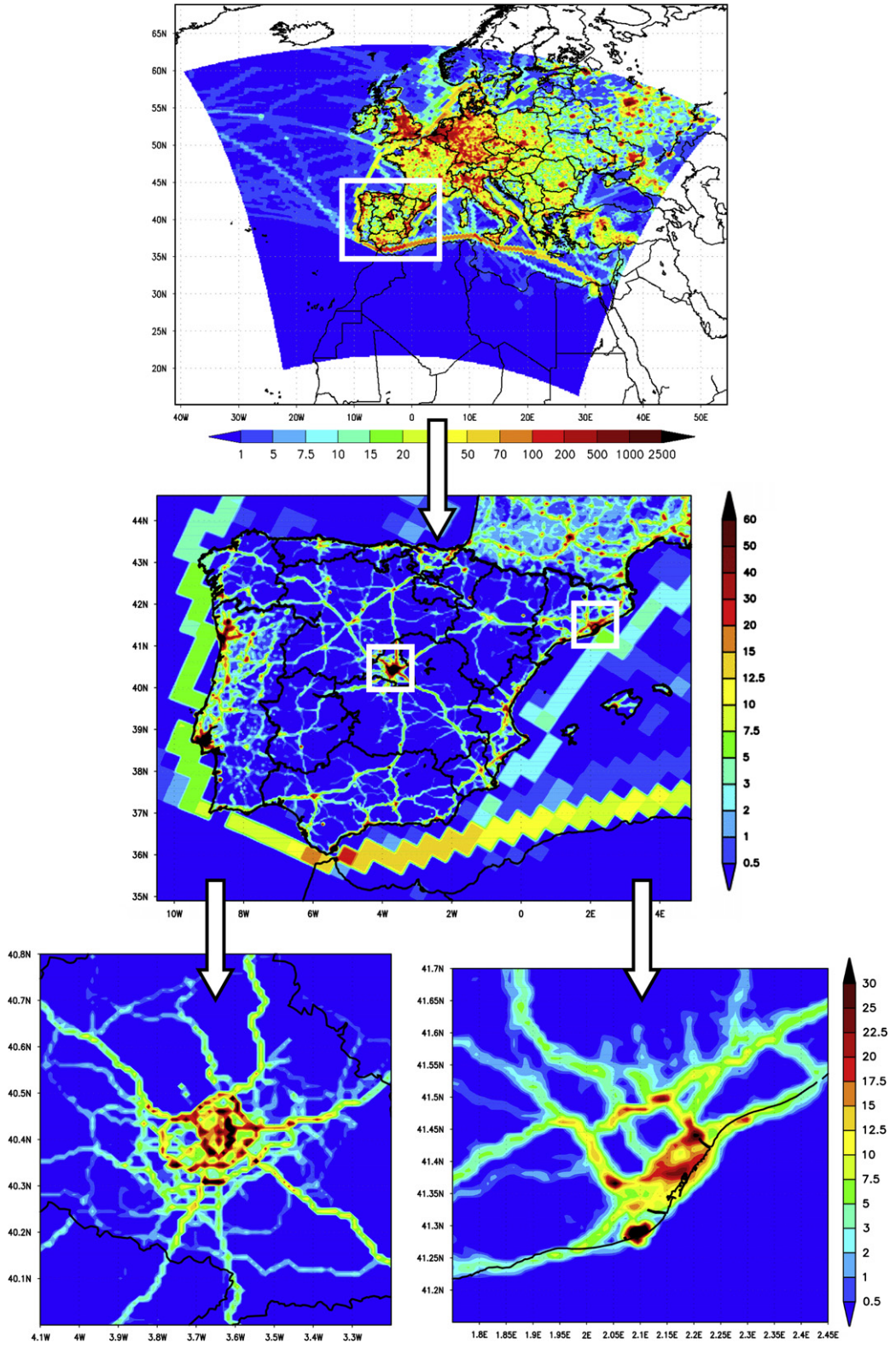

Fig. 1. Emissions for the 08 UTC, July 3, 2004, implemented within the Caliope air quality forecasting system: Europe (derived from EMEP and disaggregated to 12 km resolution, up); Iberian Peninsula (4-km resolution; estimated by HERMES for Spain and derived from EMEP for France, Portugal and maritime emissions and disaggregated to 4 km; centre); and Madrid (down-left) and Barcelona (down-right) Greater Areas (calculated with HERMES).

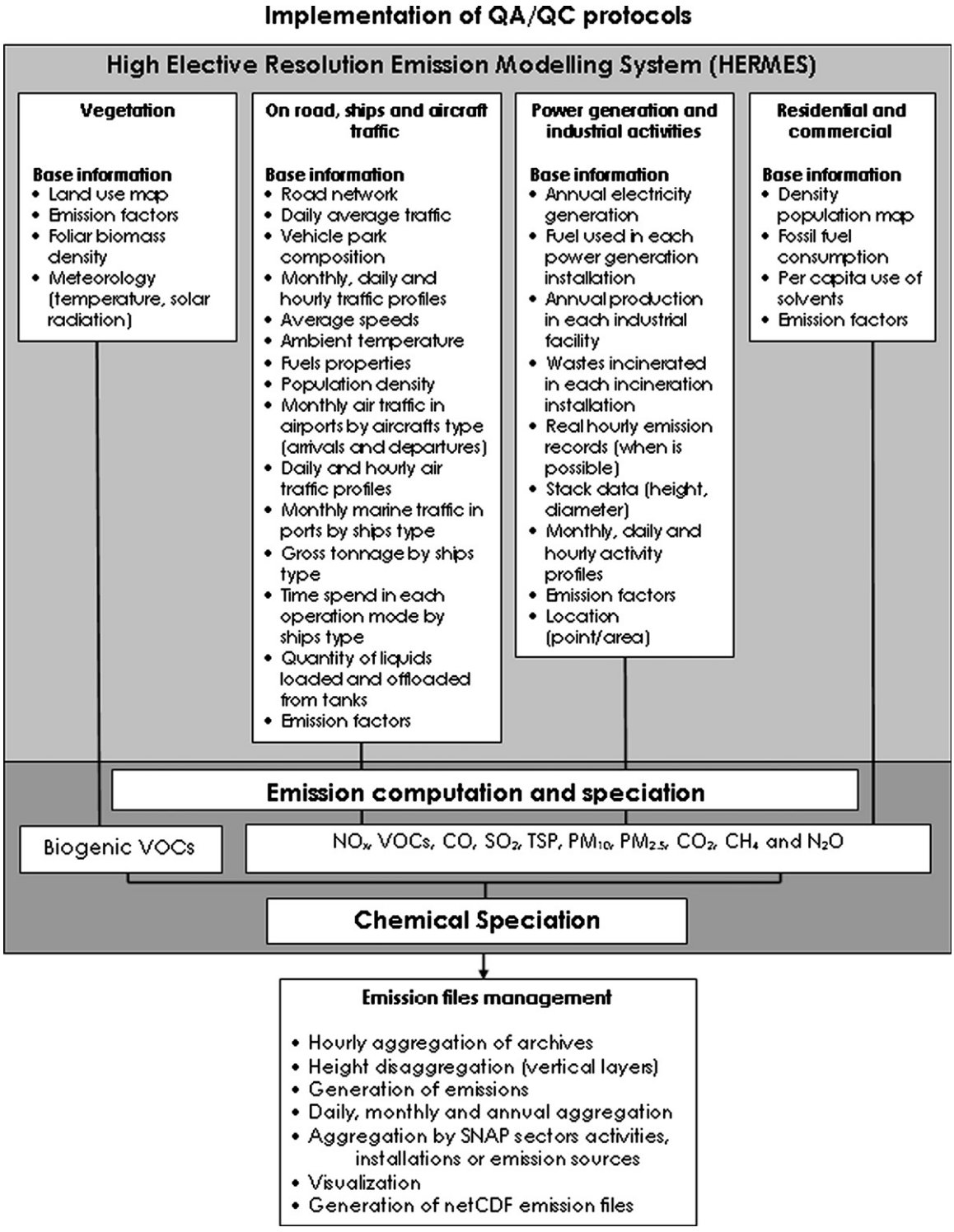

Fig. 2. Scheme of the methodology followed in the HERMES emission model framework.

base information and the emission factors that can be improved to obtain more accurate inventories. According to the information reported in Table 2, the most accurate module is on-road transport (78.1/100) followed by power generation plants (72.3/100), mainly because of the accurate information regarding emission factors, activity factors, temporal and spatial distribution (high quality of the base information). The modules containing the largest

Table 2
Summary of the information sources and methodology used within HERMES emission model

Activity/module		Quality of emission	Information sources	Methodology
Airports emissions by LTO cycle (<1000 m)		67.3	Emission factors: EMEP/CORINAIR (2005), USEPA (2005). Number of operations by plane type	EMEP/CORINAIR (2005)
Ports		62.0	Emission factors: Techne (1998) and USEPA (2000). Number of incomings and exits from each port. Time for manoeuvring: USEPA (2005). Temporal disaggregation of emissions: EMEP/CORINAIR (2005)	Techne (1998)
Biogenic		47.4	Emission factors: Gómez and Baldasano (1999) adapted by Parra et al. (2004, 2006). Land use: CORINE Land Cover 2000 map starting with a resolution of 100 m, and adapting to 22 the land-use categories according to Arévalo et al. (2004). Meteorological data: WRF simulations for the year 2004 (Jorba et al., 2008); foliar biomass density: Parra et al. (2004, 2006)	Guenther et al. (1995) adapted by Parra et al. (2004, 2006)
Domestic and commercial fossil fuel use		50.7	Emission factors: USEPA (2002); population density: Spanish National Statistics Institute (personal communication); activity factor: Spanish Ministry of Industry, Tourism and Trade (personal communication); temporal disaggregation: Costa and Baldasano (1996); Parra (2004)	USEPA (2002)
Domestic and commercial solvents use		49.3	Emission factors: EEA (2002). Population density: Spanish National Statistics Institute (personal communication); Activity data: Ministry of Industry, Tourism and Trade (personal communication, 2005); Temporal disaggregation: Parra (2004)	EEA (2002)
On-road transport		78.1	Emission factors: Ntziachristos and Samaras (2000). Measured daily average traffic: different Spanish Governmental Authorities (Central Government, Autonomous Communities, individual cities). Fleet composition: speed data: Tele Atlas Multinet™ 2005. Meteorological data: WRF simulations for the year 2004 (Jorba et al., 2008). Temporal information: Parra (2004); Parra et al. (2006)	COPERT III (Ntziachristos and Samaras, 2000)
Power generation plants		72.3	Emission factors: EEA (2004); USEPA (1996a,b,c,d, 2003); and Spanish National Office of Emission Control for Large Combustion Facilities (OCEM-CIEMAT). Activity data: Ministry of Industry, Tourism and Trade (personal communication, 2005). Temporal disaggregation: OMEL (2005a,b)	EEA (2004) and USEPA (2003)
Waste incineration		63.0	Emission factors and activity data: AEVERSU (2005). Minute information of measured emissions provided by XEAC (Catalonia Government, personal communication)	EEA (2004) and USEPA (2003)
Industrial installations	Ceramic Tile	44.7	Emission factors: EEA (2004); USEPA (1996d). Activity factor: data for production, invoicing and CO_2 emissions for different years. Location: ARDAN (2005); constant temporal profiles for production and temporal disaggregation	EEA (2004); USEPA (1996a,b,c,d, 2003)
	Lime	35.0	Emission factors: EEA (2004); USEPA (1996b); TNO (1995a). Activity factor: Spanish Ministry of the Environment Plan for the Assignment of GHGs emissions. Location: ARDAN (2005); constant temporal profiles for production and temporal disaggregation	
	Power co-generation	43.7	Emission factors: EEA (2004); USEPA (1996a,b,c). Activity data and temporal disaggregation: Ministry of Industry, Tourism and Trade (personal communication)	
	Concrete and cement	56.0	Emission factors: EEA (2004); TNO (1995b). Activity factor: total production of the sector for the year 2003. Location: EPER project; Constant temporal profiles for production and temporal disaggregation	
	Enamel and frits	46.7	Emission factors: EEA (2004) and USEPA (1997). Activity factor: Spanish Ministry of the Environment Plan for the Assignment of GHGs emissions. Location: ARDAN (2005); constant temporal profiles for production and temporal disaggregation	
	Paint	56.0	Emission factors: EEA (2004). Activity factor: Spanish Ministry of the Environment Plan for the Assignment of GHGs emissions. Location: ARDAN (2005); Constant temporal profiles for production and temporal disaggregation	
	Paper and pulp	51.3	Emission factors: USEPA (1983). Activity factor: ARDAN (2005). Location: ASPAPEL (2005); constant temporal profiles for production and temporal disaggregation	
	Refining	55.7	Emission factors: EEA (2004); USEPA (1996a). Activity factor: real production of the sector for the year 2004 reported by OILGAS. Temporal congruency based on the information by CORES reporting different monthly emissions	
	Tiles and brick	44.7	Emission factors: EEA (2004); USEPA (1996c). Activity factor: Spanish Ministry of the Environment Plan for the Assignment of GHGs emissions. Location: ARDAN (2005); constant temporal profiles for production and temporal disaggregation	
	Glass	46.7	Emission factors: EEA (2004). Activity factor: Spanish Ministry of the Environment Plan for the Assignment of GHGs emissions. Location: ARDAN (2005); constant temporal profiles for production and temporal disaggregation	

uncertainty are those related to industrial installations (lime, 35.0/100 because of the large uncertainty in the emission factors and the lime production; and power co-generation, 43.7/100 since of the temporal congruency-data available for the year 2003 and not 2004).

2.1. Power generation

The emissions inventory considers 58 power generation installations with 196 generator groups, for which total emissions are calculated after Eq. (1).

$$E_j(\text{annual}) = \text{EF}_j \cdot \text{AF} \quad (1)$$

where E_j(annual), represents the annual emissions of j pollutants in each source, AF is the activity factor on an annual basis, which can be energy consume, electricity generated or production, and EF_j is the emission factor of j pollutant, which is related to the activity factor. The emission factors were chosen mainly from EEA (2004) and USEPA (2003) and corrected by using the measured emission data provided by the Spanish National Office of Emission Control for Large Combustion Facilities (OCEM-CIEMAT) in the cases of power generation plants, where there was information available related to NO_x, SO_2 and TSP. For five generator groups in Catalonia (northeastern Spain) the hourly measured emissions record has been used according to the emission network monitoring of the Environmental Department of Catalonia Government (XEAC).

The hourly, daily and monthly emissions are calculated according to the power production profiles for 2004, reported in OMEL (2005a),(b). The emissions are spatially assigned to the coordinates and to the height where they are produced.

2.2. Industrial sources

The emissions inventory considers 1615 sources in Spain; including refineries, cement, lime, paper-mill industry, glazed ceramic, bricks and tiles, glass, paint manufacturing and chemical industry. Because of the diversity and complexity of these industrial activities, the hourly, daily and monthly emissions are calculated through temporal factors, which are estimated considering the daily operational time specific for each industrial sector. As in the case of power generation, the emissions are spatially assigned to the coordinates and to the height where they are produced.

For all the industrial activities the total emissions were calculated separately considering emissions related to the combustion and the industrial processes themselves, according to Eq. (1). Waste incineration is included here since emissions are calculated following this methodology. The emission factors were chosen mainly from EEA (2004) and USEPA (2003). For nineteen big stacks in Catalonia region the XEAC emissions were also used.

2.3. Use of fossil fuels by residential and commercial sectors

The emissions from domestic and commercial fossil fuel use are based on the statistical consumption of natural gas, liquefied petroleum gas (LPG) and diesel oil (heating), calculated for the 50 provinces of Spain. The annual emissions for this sector are calculated after Eq. (2):

$$E_{ij}(k,\ \text{annual}) = \text{EC}_j \cdot \text{EF}_{ij} \cdot \frac{P_k}{\text{Pop}} \quad (2)$$

where $E_{ij}(k$, annual) is the annual emissions of pollutant i, due to the consume of the j fossil fuel in the k cell (g year^{-1}); P_k is the human population in k cell; and Pop the total population in the studied province; EF_{ij} the emission factor for i pollutant due to the consume of j fossil fuel (g GJ^{-1}), and EC_j is the energetic consume of j fossil fuel in the province (GJ year^{-1}).

Spatial allocation was made using the population density. Temporal allocation followed the monthly, daily and hourly profiles obtained by Costa and Baldasano (1996) and Parra (2004).

2.4. Use of solvents by residential and commercial sectors

Fugitive emissions due to paint application, glues, adhesives, toiletries, propellants and car care products use are the major sources of NMVOC, which are calculated according to a top — down approach, considering the Eq. (3).

$$E_j(k,\ \text{annual}) = P_k \cdot \text{EF}_j \quad (3)$$

where $E_j(k$, annual) is the NMVOC annual emissions due to the solvent use in j activity, for the k cell (kg year^{-1}); P_k is the population in the k cell and EF_j is the emission factor per capita for the studied area due to the j activity (kg person^{-1} year^{-1}). The emission factor per capita follows EEA (2002).

Spatial allocation was made using a population density map. Monthly allocation was made considering that the paint application activity increases during spring and summer months; daily distribution considers the same consumption for each day of the week; and hourly profiles assume more activity during the morning (Parra, 2004).

2.5. Road transport

The road transport emissions are based on the daily average traffic (DAT), measured in 20,934 observation points throughout Spain, generating a digital vector map where all the highways, freeways, more important roads (DAT >200); and for large cities with over 500,000 inhabitants (Madrid, Barcelona, Valencia, Saragossa, Seville and Malaga) urban streets are also considered. The speed data needed for emission estimation consist of 372,640 road stretches (among which 115,638 are urban stretches) adding up to 118,087 km with information (10,003 km within cities) provided by Tele Atlas Multinet™ 2005.

Three types of emissions were included: (1) hot exhaust emissions, occurring under thermally stabilised engine and exhaust after treatment conditions; (2) cold exhaust emissions, occurring during transient thermal engine operation (cold start); and (3) evaporative emissions, non-exhaust volatile organic compounds (VOC) emissions relevant for gasoline fleet. Also, non-exhaust particles emissions (tire and brake wear, road abrasion) are included within HERMES

and follow the methodology described by the Coordinated European Program on Particulate Matter Emission Inventories, Projections and Guidance (CEPMEIP, 2008).

The inventory considers the 2004 vehicular park composition, distinguishes between working days and weekend, and is based on the COPERT III model (Ntziachristos and Samaras, 2000), according to which the total emissions for each pollutant are calculated (Eq. (4)).

$$E^{\mathrm{itot}}(k,\mathrm{hourly}) = \sum_r E_r^{\mathrm{ihot}}(k,\mathrm{hourly}) + \sum_r E_r^{\mathrm{icold}}(k,\mathrm{hourly}) + E^{\mathrm{evap}}(k,\mathrm{hourly}) \quad (4)$$

where $E^{\mathrm{itot}}(k,\mathrm{hourly})$ is the total emissions of i-pollutant in k-cell, hourly (g h^{-1}); $E_r^{\mathrm{ihot}}(k,\mathrm{hourly})$, the hot exhaust emissions of i-pollutant in the road section r of k-cell per hour (g h^{-1}); $E_r^{\mathrm{icold}}(k,\mathrm{hourly})$ is the cold emissions of i-pollutant in the road section r of k-cell per hour (g h^{-1}); and $E^{\mathrm{evap}}(k,\mathrm{hourly})$ the evaporative emissions in the k-cell per hour (g h^{-1}).

The hot exhaust emissions of i-pollutant in the road section r of k-cell per hour are calculated with Eq. (5):

$$E_r^{\mathrm{ihot}}(k,\mathrm{hourly}) = \mathrm{Crh}\cdot\sum_{j=1}^{n}\mathrm{Clf}\cdot\mathrm{Crd}\cdot\mathrm{DAT}_{rj}(k)\cdot L_r(k)\cdot F_j^{\mathrm{ihot}}(s_r) \quad (5)$$

where Crh is the proportion of DAT at h-hour; Clf, the coefficient for daily traffic (working day or weekend); Crd is the ratio between daily traffic for a specific month and DAT; $\mathrm{DAT}_{rj}(k)$ is the daily average traffic for r-road section and j-vehicle category in k-cell (number of vehicles); $L_r(k)$ represents the length of the road section r in k-cell (km); $F_j^{\mathrm{ihot}}(s_r)$ is the hot emission factor (g km^{-1}) of the pollutant i for the vehicle category j, related to the speed S_r on the road section r; and n (72) is the number of vehicle categories considered.

Hourly emissions are based on the hourly coefficients (Crh), which are calculated with the hourly distribution of the DAT, provided by the Governmental Authorities. Monthly and annual emissions were obtained adding up their respective daily and monthly values.

Cold emissions are produced mainly in urban streets for all the vehicle categories; however only gasoline and diesel cars are considered. These emissions are added to hot emissions and are calculated by Eq. (6):

$$E_r^{\mathrm{icold}}(k,\mathrm{hourly}) = \sum_{j=1}^{n} E_r^{\mathrm{ihot}}(k,\mathrm{hourly})\cdot\beta(\mathrm{ltrip},at)\cdot\left(\frac{F_j^{\mathrm{icold}}}{F_j^{\mathrm{ihot}}}(at)-1\right) \quad (6)$$

where $\beta(\mathrm{ltrip}at)$ is the fraction of the route driven with cold engines, based on the average trip length and ambient temperature at; and $F_j^{\mathrm{icold}}/F_j^{\mathrm{ihot}}(at)-1$ is the cold over hot ratio of i-pollutant emission, also related to at.

Evaporative emissions include three kinds of sources: (1) diurnal emissions; (2) soak emissions; and (3) running losses.

Diurnal emissions are produced for the daily ambient temperature variation, which result in vapours' expansion inside the gasoline tank. According to Ntziachristos and Samaras (2000), it is actually only possible to estimate the evaporative emissions for gasoline cars and motorcycles, which are denominated as category m of the total vehicles fleet. Total daily diurnal emissions are calculated using Eq. (7):

$$E_{\mathrm{m}}^{\mathrm{devap}}(k,\mathrm{hourly}) = (1/24)\cdot(at/\mathrm{atm})\cdot N_{\mathrm{m}}\cdot e_{\mathrm{m}}^{\mathrm{d}}(t_{\max},t_{\min},\mathrm{RVP}) \quad (7)$$

where $E_{\mathrm{m}}^{\mathrm{devap}}(k,\mathrm{hourly})$ is the evaporative diurnal emissions produced for vehicles of m-category (g h^{-1}); at is the ambient temperature at that hour; atm the daily average ambient temperature; N_{m}, is the number of vehicles of the m-category in the k-cell which generates evaporative diurnal emissions; and $e_{\mathrm{m}}^{\mathrm{d}}$ is the diurnal emission factor (g day^{-1}) for m-category vehicles in function of maximum and minimum ambient temperature and gasoline volatility (RVP) on that day.

Soak emissions are produced when the hot engine is turned off and the temperature of the stagnant fuel increases. There are two types of soak emissions: warm soak and hot soak emissions. The total daily soak emissions are calculated by Eq. (8):

$$E_{\mathrm{m}}^{\mathrm{sevap}}(k,\mathrm{hourly}) = (1/24)\cdot(at/\mathrm{atm})\cdot N_{\mathrm{m}} \times\left(p\cdot x_{\mathrm{m}}\cdot e_{\mathrm{m}}^{\mathrm{shot}}(at,\mathrm{RVP})\right) + w\cdot x_{\mathrm{m}}\cdot e_{\mathrm{m}}^{\mathrm{swarm}}(at,\mathrm{RVP}) \quad (8)$$

where $E_{\mathrm{m}}^{\mathrm{sevap}}(k,\mathrm{hourly})$ is the evaporative soak emissions produced by the m vehicles category (g h^{-1}); at is the ambient temperature at that hour; atm the daily average ambient temperature; N_{m} is the number of vehicles in m-category; p is the fraction of trips finished with a hot engine; w the fraction of trips finished with cold or warm engine ($p+w=1$); x_{m} is the mean number of trips for m-category vehicles, $e_{\mathrm{m}}^{\mathrm{shot}}(at,\mathrm{RVP})$ the emission factor for hot soak emissions (g trip^{-1}) for m-category of vehicles in function of ambient temperature and gasoline volatility; and $e_{\mathrm{m}}^{\mathrm{swarm}}(at,\mathrm{RVP})$ is the emission factor for cold or warm soak emissions for m-category of vehicles in function of ambient temperature and gasoline volatility (g trip^{-1}).

Running losses are produced from fuel evaporation in the tanks during vehicle operations. There are also warm and hot emission factors much alike the soak ones, but disaggregation is calculated using equivalent equations as the hot exhaust emissions.

2.6. Ports

In the estimation of emissions for port traffic the 50 harbours with mercantile activities in Spain are considered individually. The inventory is based on Techne (1998) methodology, considering the emissions generated by each of the next operation modes: (1) manoeuvring: includes the operations of entrance and exit to harbour (in this model is considered 1 nautical mile of distance); (2) hotelling refers to the stay of the ship in the harbour where emissions are generated due to lighting, heating, refrigeration, ventilation, etc.; and (3) tank offloading and loading. The emissions are calculated using Eq (9):

$$E_{ip}(\text{annual}) = E_{ip}^{\text{man}}(\text{annual}) + E_{ip}^{\text{har}}(\text{annual}) \quad (9)$$

where E_{ip}(annual)is the annual emission of i-pollutant for port p (kg); E_{ip}^{man}(annual) is the annual emission of i-pollutant in port p, due to manoeuvring mode (kg) and E_{ip}^{har}(annual)is the annual emission of i-pollutant in the dock of p-port, including hotelling (E_{ip}^{hot}(annual)) and tanks load and offload (E_{ip}^{l}(annual)) emissions, according to Eq. (10):

$$E_{ip}^{\text{har}}(\text{annual}) = E_{ip}^{\text{hot}}(\text{annual}) + E_{ip}^{l}(\text{annual}) \quad (10)$$

Emissions generated by manoeuvring and hotelling modes are calculated each with Eq. (11), using the emissions factors defined by Techne (1998) and USEPA (2000), corresponding to each operation mode (o, meaning hotelling or manoeuvring).

$$E_{ip}^{o}(\text{annual}) = \sum_{b} C_{bp}(GT_{bp}^{*}) \cdot N_{bp} \cdot FC_{bo} \cdot T_{bop} \cdot EF_{icto} \quad (11)$$

where $C_{bp}(GT_{bp}^{*})$is the fuel consumption at top speed for ship type b in port p, in function of the mean gross tonnage (t day^{-1}); N_{bp} the number of type b ships in port p (annual basis); $FC_{bo}$is the fraction of fuel used according to the operation mode o (hotelling or manoeuvring) of the type b ship; T_{bop} is the time spent in each operation mode (hotelling or manoeuvring) (days); and EF_{icto} is the emission factor of i-pollutant, considering type of fuel used, type of engine and operation mode (hotelling or manoeuvring) (kg t^{-1} of fuel).

Emissions generated by loading and offloading of tank ships are calculated with Eq. (12):

$$E_{ip}^{l}(\text{annual}) = \left(\frac{L_p \cdot c}{1000}\right) \cdot EF_i^{l} \quad (12)$$

where L_p is the quantity of liquids loaded and offloaded annually of tank ships in port p (t); c corresponds to the fuel used for the cargo pumps for tanker loading and offloading (0.7 kg t^{-1} according to Scott Environmental Technology, 1981); and EF_i^{l} is the emission factor of i-pollutant for tank offloading and loading (kg t^{-1} of fuel).

The spatial allocation distinguishes between harbour and manoeuvring emissions. In the first case emissions are allocated into the cells included total or partially in the port area; the manoeuvring emissions are proportionally allocated into the marine surface of the cells enclosed by a 1 nautical mile radius circle centred at the central point of the port.

Hourly and daily emissions allocation consider a constant activity profile for each port, meanwhile monthly emissions are calculated through monthly factors, which are estimated considering the monthly operations in each port.

2.7. Airports

Emissions from aircrafts were estimated according to the number of landing and take-off cycles (LTO) at each of the 44 airports with civil aviation in Spain. The model considers the type of airplane and the emission factor for each of the five operation phases of the LTO cycle: final approach, taxi-in, taxi-out, take-off and climb out, according to the EMEP/CORINAIR guidebook (2005).

The emissions are calculated with monthly data according to Eq. (13).

$$E_{ia}(\text{monthly}) = \sum_{s} \sum_{t} N_{atm} \cdot FE_{ist} \quad (13)$$

where E_{ia}(monthly) is the monthly emission of i-pollutant in airport a (g); N_{atm} is the number of operations in airport a, by aircraft type t in month m; and FE_{ist} is the emission factor of i-pollutant for operation phase s and aircraft type t (g per operation phase).

The annual emissions are obtained adding up the monthly values; daily and hourly emissions are calculated applying a coefficient of daily and hourly air traffic.

Spatial allocation is accomplished by georeferencing the landing strip and the airport area considering the LTO phases. Taxi-in and taxi-out emissions are distributed into the airport area cells (at ground level) while take-off emissions are distributed into the cells crossed by the strips proportionally to its length (also at ground level). The emissions of final-approach and climb-out are allocated on a 3D basis distributing the total value proportionally into the cells crossed by a lineal trajectory outlined between the (last or first) contact point in the strip and 1000 m of altitude according to the angle of elevation or descent in that strip.

2.8. Biogenic emissions

The emission inventory calculates the volatile organic compounds from vegetation, which are grouped in three categories according to their reactivity: isoprene, monoterpenes and other volatile organic compounds (OVOC). The model considers the influence of temperature and photosynthetically active radiation (PAR) by the Guenther et al. (1995) algorithms, according to Parra et al. (2004), (Parra et al., 2006).

Hourly isoprene emissions were estimated using Eq. (14):

$$E_{\text{iso}}(k, \text{hourly}) = EF_j^{\text{iso}} \cdot ECF(t,p) \cdot FB_j \cdot A_k \quad (14)$$

where $E_{\text{iso}}(k, \text{hourly})$ is the hourly isoprene emission into the k-cell (g h^{-1}), EF_j^{iso} is the standard isoprene emission factor associated with the j land-use category (g g^{-1} h^{-1}), $(ECFt, p)$ is the environmental correction factor owing to temperature and PAR (a dimensional), FB_j is the foliar biomass density of the j land-use category (g m^{-2}) and A_k is the area of each grid cell (m^2).

The environmental correction factor is calculated using Eq. (15):

$$ECF(t,p) = C_t \cdot C_p \quad (15)$$

Where C_t is the correction factor owing to temperature and C_p is the correction factor due to PAR, which are calculated according to Eqs. (16) and (17), respectively.

$$C_t = \frac{\exp \frac{C_{T1}(T-T_s)}{RT_sT}}{1 + \exp \frac{C_{T2}(T-T_m)}{RT_sT}} \quad (16)$$

$$C_p = \frac{\alpha . C_{L1} L}{\sqrt{1 + \alpha^2 L^2}} \quad (17)$$

where C_{T1} (95,000 J mol^{-1}), C_{T2} (230,000 J mol^{-1}), T_m (314 K), α (0.0027) and C_{L1} (1.066) are empirical coefficients. T_s is the standard reference temperature (303 K), R (8.314 J K^{-1} mol^{-1}) is the universal gas constant, T (°C) is the foliar biomass temperature (it is assumed that foliar biomass temperature is similar to the surface air temperature) and L is the PAR flux (μmol m^{-2} s^{-1}).

Hourly monoterpenes emissions were estimated using Eq. (18):

$$E_{\mathrm{mon}}(k,\mathrm{hourly}) = EF_j^{mon} \cdot M(t) \cdot FB_j \cdot A_k \quad (18)$$

where $E_{\mathrm{mon}}(k,hourly)$ is the hourly monoterpenes emission into the k-cell (g h^{-1}) and EF_j^{mon} is the monoterpenes emission factor related to the j land use category (g g^{-1} h^{-1}). $M(t)$ is the environmental correction factor based on temperature (a dimensional) which is calculated by Eq. (19).

$$M(t) = \exp(\beta^*(T - T_s)) \quad (19)$$

where β is an empirical coefficient (0.09 K^{-1}).

The hourly OVOCs emissions were estimated according to the Eq. (18) used to calculate hourly monoterpene emissions.

The land-use categories for each grid cell are obtained from CORINE Land Cover 2000 map starting with a resolution of 100 m, and adapting to 22 the land-use categories according to Arévalo et al. (2004).

3. Results and discussion

One of the capabilities of HERMES is the generation of results according SNAP sectors. Therefore, the emission sources have been split according to the SNAP codes at the highest existing level (when possible) and then aggregated in 9 of the 11 SNAP codes: 01) combustion in energy and transformation industries; 02) non-industrial combustion plants; 03) combustion in manufacturing industry; 04) production processes; 06) solvent and other product use; 07) road transport; 08) other mobiles sources and machinery; 09) waste treatment and disposal; and 11) other sources and sinks.

3.1. Total annual emissions

The total annual emissions are presented in Fig. 3 and Table 3, and also in Fig. 4, where the spatial distribution is illustrated. These annual emissions are obtained by aggregation of the emissions corresponding to each of the individual hours of the year 2004, since the calculation basis of HERMES model refers to 1 h.

The annual emissions of primary air pollutants add up to 4379 kt, distributed as: NO_x, 795 kt (18%); NMVOC, 1025 kt (23%); CO, 1236 kt (28%); SO_2, 1142 kt (26%) and TSP, 180 kt (4%) (Fig. 3a).

Fig. 3b illustrates the percentage of emissions generated by each SNAP sector; for NO_x the most significant sources are combustion in energy and transformation industries (SNAP 01) (41%), the road transport (SNAP 07) (37%) and combustion in manufacturing industries (SNAP 03) (15%). Consequently, Fig. 4a shows that NO_x highest values (>22,600,000 kg year^{-1} cell^{-1}) are located in cells where

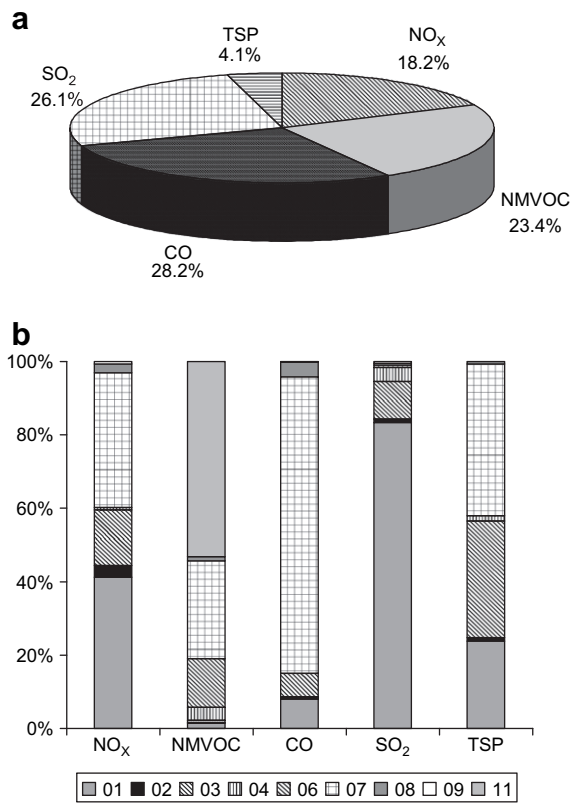

Fig. 3. Total annual emissions calculated by HERMES for Spain 2004; (a) percentual composition of the emissions, (b) contributions by SNAP sectors.

power generation plants and industrial installations are located; in the main cities, principally in Madrid and Barcelona (>2,840,000 kg year^{-1} cell^{-1}), and in the principal highways.

The NMVOC (Fig. 3b) are principally generated by vegetation (SNAP 11) (53%), road traffic (SNAP 07) (27%) and solvent and other product uses (SNAP 06) (13%). In Fig. 4b the highest values (>1,750,000 kg year^{-1} cell^{-1}) correspond to the largest cities due to the consideration of evaporative emissions from road traffic and the use of solvents by residential and commercial sectors (included in SNAP 06). The biogenic emissions are distributed by almost all the territory with emission values between 5700 and 18,500 kg year-cell^{-1}, which explains the important contributions of the vegetation to the total NMVOC.

In the case of CO, 81% of the emissions correspond to road traffic (SNAP 07), 8% to combustion in energy and transformation industries (SNAP 01) and 6% to combustion in manufacturing industries (SNAP 03) (Fig. 3b). The spatial distribution of CO (Fig. 4c) shows that the highest emission levels (>5,611,000 kg year^{-1} cell^{-1}) are generated in medium and large cities and highways due to the emissions from road transport and to the use of fossil fuels by residential and commercial sectors (in the cities) and in energy generation and industrial plants.

TSP are mainly emitted by road traffic (SNAP 07) (41%), combustion in manufacturing industry (SNAP 03) (32%) and

Table 3
Comparison of emissions calculated by HERMES and Spanish National Emission Inventory (SNEI) for the year 2004

SNAP sector	NO_x (kt year^{-1})			NMVOC (kt year^{-1})			CO (kt year^{-1})			SO_2 (kt year^{-1})			TSP (kt year^{-1})		
	HERMES	SNEI	Dif	HERMES	SNEI	Dif	HERMES	SNEI	Dif	HERMES	SNEI	Dif	HERMES	SNEI	Dif
01	328	311	17	15	8	7	99	22	77	952	1004	−52	43	35	7
02	25	49	−23	1	40	−39	8	491	−483	12	32	−20	2	27	−25
03	121	285	−165	7	23	−17	79	172	−93	115	188	−73	57	21	36
04	4	12	−8	36	211	−175	0	409	−409	45	41	4	3	12	−10
06				136	487	−351									
07	293	505	−212	273	190	84	1000	1033	−33	7	13	−6	75	44	31
08	19	239	−220	11	30	−19	49	70	−21	6	34	−28	1	44	−43
09	5	9	−4	0	28	−28	1	80	−79	5	15	−10	0	7	−7
11				545	1201	−655									
Total	795	1450	−654	1025	2219	−1193	1236	2441	−1205	1142	1328	−185	180	190	−10

combustion in energy and transformation industries (SNAP 01) (24%) as shown in Fig. 3b. The spatial distribution of TSP focuses on particles with a diameter under 2.5 μm because of their special implications for human health. They are associated with the increasing of mortality, especially from cardiovascular and cardiopulmonary diseases (Pope et al., 2002). Fig. 4d shows that the highest emission levels of $PM_{2.5}$ are displayed in cells with power generation installations and industrial plants (>1,600,000 kg year^{-1} cell^{-1}), followed by main cities urban areas (>86,000 kg year^{-1} cell^{-1}) due principally to the road transport, which besides provokes emissions along the highways axes and highways (>1900 kg year^{-1} cell^{-1}).

Regarding SO_2, 83% is generated by combustion in energy and transformation industries (SNAP 01); 10% by combustion in manufacturing industries (SNAP 03) and 4% by production processes (SNAP 04) (Fig. 3b). Fig. 4e shows that the highest levels of SO_2 (>77,000,000 kg year^{-1} cell^{-1}) are presented in isolated cells where power generation facilities and manufacturing industries are located. Furthermore, large cities depict emissions levels over 91,000 kg year^{-1} cell^{-1} caused principally by the use of fossil fuels by residential and commercial sectors (considered in SNAP 02) and industrial installations located in the outskirts and suburban areas.

The comparison of HERMES emissions with other emissions inventories permits to have a reference of the estimations made with the model, albeit these inventories are based on different estimation methodologies. In this sense, the most reliable emission inventory for the area of study of HERMES is the Spanish National Emission Inventory (SNEI), which is the base of the Spanish contribution to the EMEP inventory and is publicly available.

The comparison shows that estimates for HERMES are lower than those in the SNEI for almost all the sectors, except SNAP 01 (Table 3). The grade of similarity varies between different sources categories and pollutants. The comparison of the total annual emissions show that TSP presents the minimum difference between HERMES and NEI (−10 kt year^{-1}), while CO represents the highest deviation in the comparison (−1205 kt year^{-1}). The sectorial comparison shows that the smallest differences for NO_x are found in SNAP 09 (−4 kt year^{-1}), for NMVOC in SNAP 01 (7 kt year^{-1}), for CO in SNAP 08 (−21 kt year^{-1}), for SO_2 in SNAP 04 (4 kt year^{-1}) and for TSP in SNAP 09 (−7 kt year^{-1}) (Table 3).

According to Lindley et al. (2000), the reasons for the differences between different inventories may be caused by the differences in activity data, assumptions and emission factors considered in each estimation. In this sense, the most significant differences in SNAP 01 correspond to CO (77 kt year^{-1}), which may be originated by the use of high emissions factors of CO used in HERMES.

For SNAP 02, 03, 04, 06, 08 and 09; HERMES calculates lower emissions than SNEI for almost all the pollutants because the former does not consider all the activities involved in the SNAP codes which are included in SNEI (as the combustion plants used in agriculture, forestry and aquaculture for SNAP 02; the process in iron and steel industries and collieries in SNAP 04 or the railways and

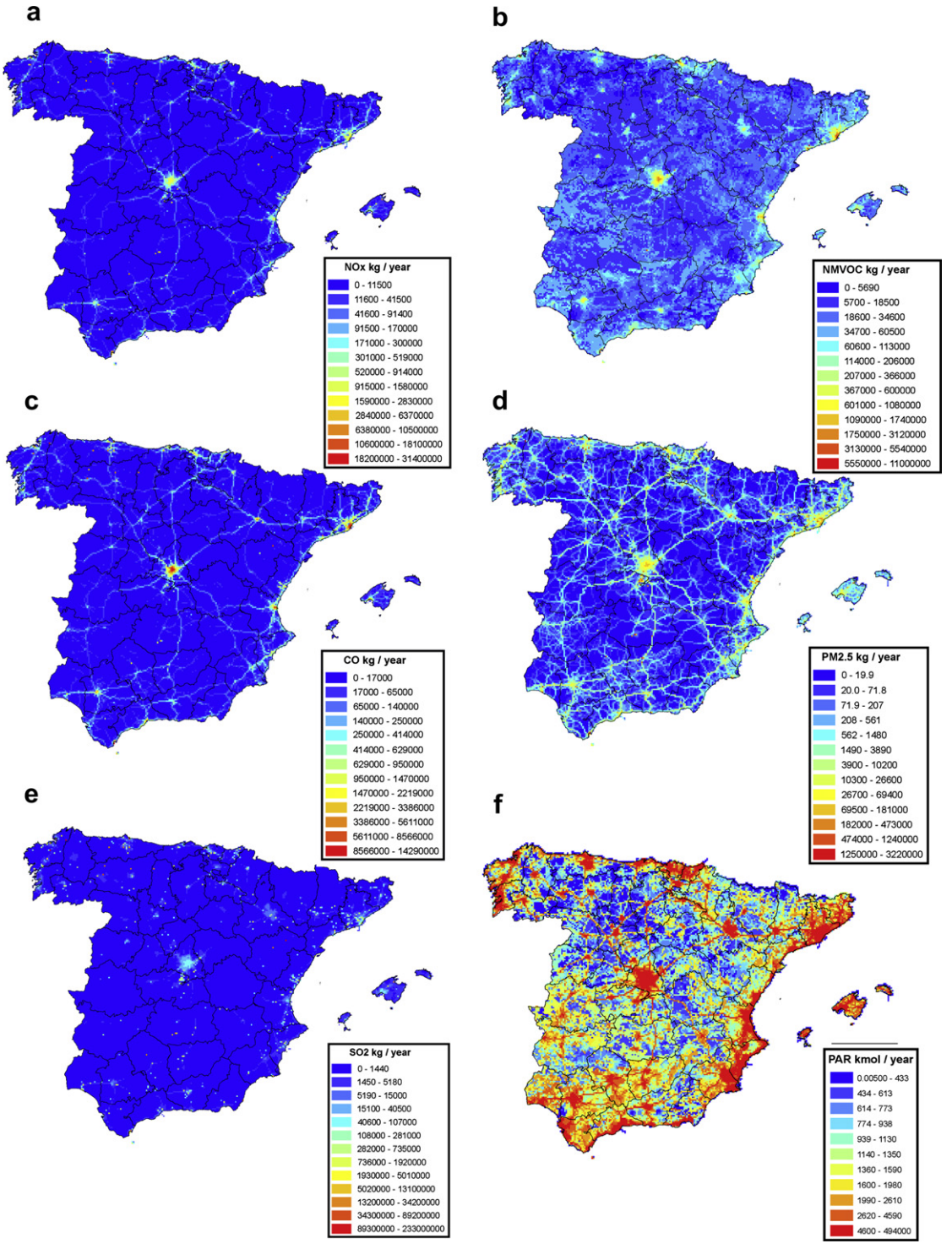

Fig. 4. Spatial distribution of the total annual emissions (kg year^{-1} cell^{-1}); (a) NO_x, (b) NMVOC, (c) CO, (d) $PM_{2.5}$, (e) SO_2, and (f) speciated species PAR (kmol year^{-1} cell^{-1}) according to CB-IV mechanism.

mobile source used in agriculture, forestry and industry in SNAP 08).

For SNAP 07 the most significant differences correspond to NO_x (-212 kt year^{-1}), which may be caused by the level of detail used in HERMES because of the lack of information regarding the calculation of emissions for small roads (DAT <200) and small and medium cities ($<500{,}000$ inhabitants).

3.2. Daily variations of emissions

Total daily emissions of CO, NMVOC, NO_x, SO_2 and $PM_{2.5}$, are illustrated in Fig. 5. CO presents a regular trend during the year with a slight increase in emissions from July 1 to August 31 due to the summertime holidays; furthermore CO trend shows higher emissions during weekdays and lower emission levels during the weekends, according to the weekday/weekend variation of traffic profiles (Jiménez et al., 2005). It also depicts the influence of road traffic emissions (SNAP 07) in this pollutant showed in Fig. 3b.

NO_x presents a similar trend to CO, with marked weekly cycles (Fig. 5) generated by the road traffic emissions (SNAP 07) and the combustion in manufacturing industries (SNAP 03), presenting higher emissions during the weekdays and lower at weekends. However, in this case the processes of combustion in energy and transformation industries (SNAP 01) also have an important contribution. The irregularities in the weekly cycle are caused by the quantity of power generated by different fuels (coal, fuel, gas) because each fuel has different emissions factors associated. The emissions of SO_2 present significant variations related to the daily power demand and the electricity mix used, showing higher emissions during weekdays and lower at weekends (Fig. 5).

The daily trend for the year 2004 of NO_x, SO_2 and $PM_{2.5}$ is similar, presenting two significant drops: during the firsts days of the year due to the decrease in power generation for holidays and during spring, because of the decrease of power generation levels due to the rise of light hours and the diminishing of heating and cooling systems due to the pleasant temperatures in the domain studied. The use of coal as a fuel for the power production determines in an important amount the daily quantity of NO_x, SO_2 and $PM_{2.5}$ emitted, the correlation levels identified are 0.64 for NO_x, 0.96 for SO_2 and 0.61 for $PM_{2.5}$ (Fig. 6a–c). The daily emission rate for $PM_{2.5}$ is lower than for the rest of pollutants (Fig. 5). Their variability is significant for some periods of the year (Fig. 6c) originated by the daily power generation using coal (SNAP 01), the combustion in manufacturing industries (SNAP 03) and road traffic (SNAP 07).

The general trend of NMVOC emissions is also showed in Fig. 5. During wintertime this pollutant reaches the minimum level of emissions while during summer it becomes maximum due to the influence of temperature and solar radiation in the biogenic NMVOC formation. This fact can be observed in Fig. 7a where the peaks and falls of NMVOC along the year are related with the variability of both temperature and solar radiation. Fig. 7b,c shows an exponential correlation between temperature ($r = 0.90$) and solar radiation with NMVOC ($r = 0.67$). The summertime variability in NMVOC emissions observed in Fig. 7a may exert a great influence on the ozone production (Meleux et al., 2005; Wei et al., 2007).

3.3. Hourly variations of emissions

In order to illustrate the HERMES capability for the estimation of emissions on an hourly basis, Fig. 8 shows a comparison between summer and winter hourly emission profiles. The summer day corresponds to Monday July 26, because this day is representative of a typical summertime episode of air pollution in southwestern Europe (according to the criteria defined in Jiménez et al., 2006) for the year 2004 and presents high emission levels; and the winter day is Monday January 19, related to a wintertime anticylonic situation over Spain.

For CO emissions (Fig. 8a), the daily major contribution is issued from road traffic (SNAP 07), with larger contributions for July 26 with respect to January 19 due to the increase of road traffic during the summer period. Emissions from other mobile sources and machinery (SNAP 08), combustion in manufacturing industry (SNAP 03) and

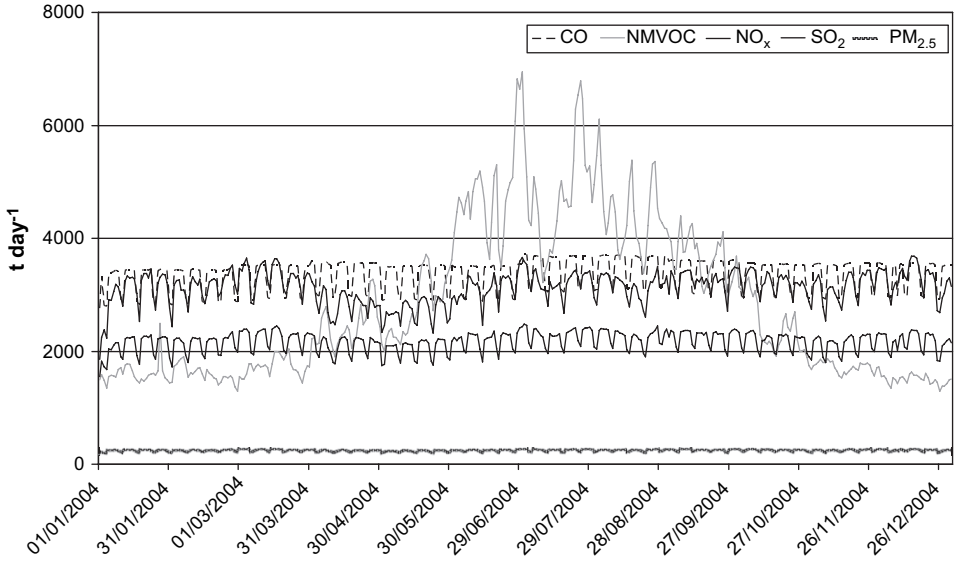

Fig. 5. Total daily emissions for Spain (t day^{-1}) estimated with HERMES model for the year 2004.

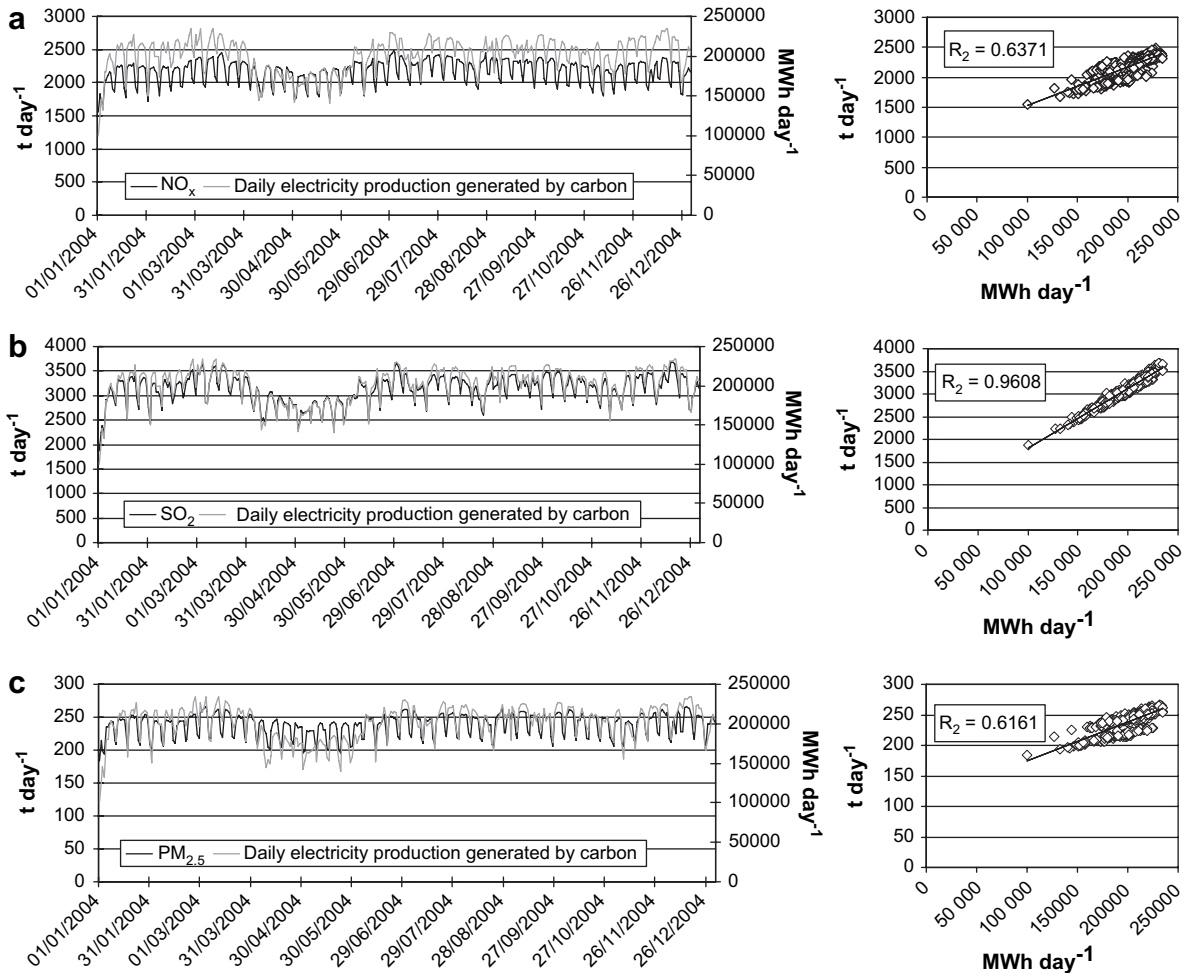

Fig. 6. Comparison between daily emissions for different pollutants (t day^{-1}) and daily electricity produced by coal (MWh day^{-1}) in Spain 2004 (left) and their correlation (right); (a) NO_x; (b) SO_2; (c) $PM_{2.5}$ (source of electricity production: OMEL, 2005b).

combustion in energy production (SNAP 01) are similar for both days. During the day three peaks are showed related with the rush hours: one at 06 Universal Time Coordinate (UTC) in summer and 07 UTC in winter, related with the displacement to work places; another one at 11 UTC in summer and 12 UTC in winter due to the mobility for the lunch time; and the third between 16 and 17 UTC in summer and between 17 and 18 UTC in winter, because of the end of the working day. The forward of 1 h between January 19 and July 26 is caused by the daylight saving time (DST) used in the summer, when the local official time in Spain is UTC + 2.

The hourly distribution of NMVOC is quite different between winter and summer days because of the large contributions of vegetation during July 26 (SNAP 11). These biogenic emissions have been increased due to the high temperatures (up to daily means of 27 °C) and intense solar radiation during summer (François et al., 2005; Parra et al., 2006). These high temperatures also generate slightly higher emissions in summer issued from evaporation processes in solvent and other products use (SNAP 06) and road traffic (SNAP 07) (Fig. 8b).

NO_x and $PM_{2.5}$ emissions are higher during the summer day due principally to the increase of two activities: the combustion in energy production (SNAP 01) associated with the rise of electricity used for cooling systems and the increase of road traffic (SNAP 07) during the summer holidays. Emissions from non-industrial combustion plants (SNAP 02) are larger in the winter day, due to the high domestic and commercial fossil fuels consume in heating systems. NO_x emissions from combustion in manufacturing industry (SNAP 03) and from other mobile sources and machinery (SNAP 08) are similar for both analyzed days because the temporal distribution of this activity sector is not greatly month- or day-dependant (Fig. 8c,d).

The hourly NO_x and $PM_{2.5}$ emissions profile for July 26 and January 19 are defined by the intensity of road traffic (SNAP 07) and combustion in energy production (SNAP 01); therefore the day emissions are higher showing two peaks related to the increase of these activities. During the summer day the emissions are skipped 1 h due to the DST.

Regarding $PM_{2.5}$ it is important to notice that production process (SNAP 04), principally point sources associated with petroleum products processing, contribute to the

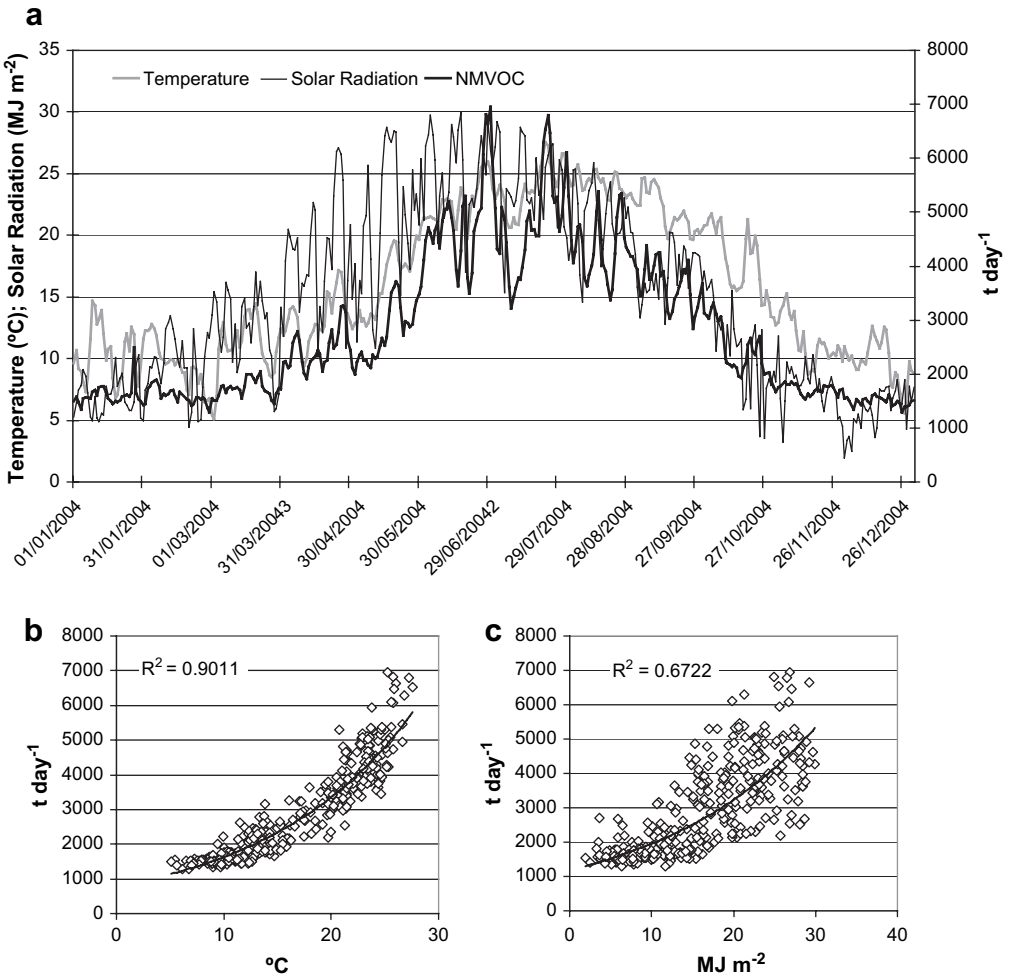

Fig. 7. (a) Comparison between daily means of temperature (°C), solar radiation (MJ m^{-2}) (both average for the entire domain) and total NMVOC emissions for Spain (t day^{-1}); (b) correlation between daily temperature means and NMVOC emissions; (c) daily solar radiation means and NMVOC emissions.

emissions levels in an equivalent way for all the hours of the year because their activity levels remain constant throughout the year.

SO_2 emissions are principally generated by combustion in energy production (SNAP 01), therefore the temporal and hourly variations are correlated with the power demand. The hourly variations for July 26 show a peak around noon (11 UTC) because this is an hour with intense labour activities which require electricity and in addition the use of cooling systems becomes necessary. January 19 presents two differentiated emission peaks, 11 UTC generated by the labour activities and at 20 UTC due to the use of artificial light systems (Fig. 8e).

4. Conclusions

This work describes the main elements and detailed results obtained with the high spatial (1 km^2) and temporal (1 h) resolution HERMES emission model as implemented within the Caliope air quality forecasting system for Spain (http://www.bsc.es/caliope) supported by the Spanish Ministry of the Environment. HERMES does not only provide detailed emission information for its coupling with chemistry transport models, but also provides the capability of performing several calculations of the emissions such as spatial and temporal aggregations, SNAP summations or aggregation by emissions sources or stacks.

The results of the application of HERMES to Spain for the entire year 2004 by the adding of the emissions calculated on an hourly basis show that the most significant sources of pollution are combustion in power generation plants (principally when coal is used as fuel), combustion in manufacturing industries, road traffic and biogenic sources. The contributions of other activity sectors are not significant. All the primary air pollutants are generated principally in the biggest urban centres and in principal highways, although biogenic NMVOC emissions are distributed around all the Spanish geography according to the high variability and heterogeneity in the distribution of vegetation and land use.

The daily annual emission distribution presents a similar pattern for NO_x, CO and particulate matter with weekly

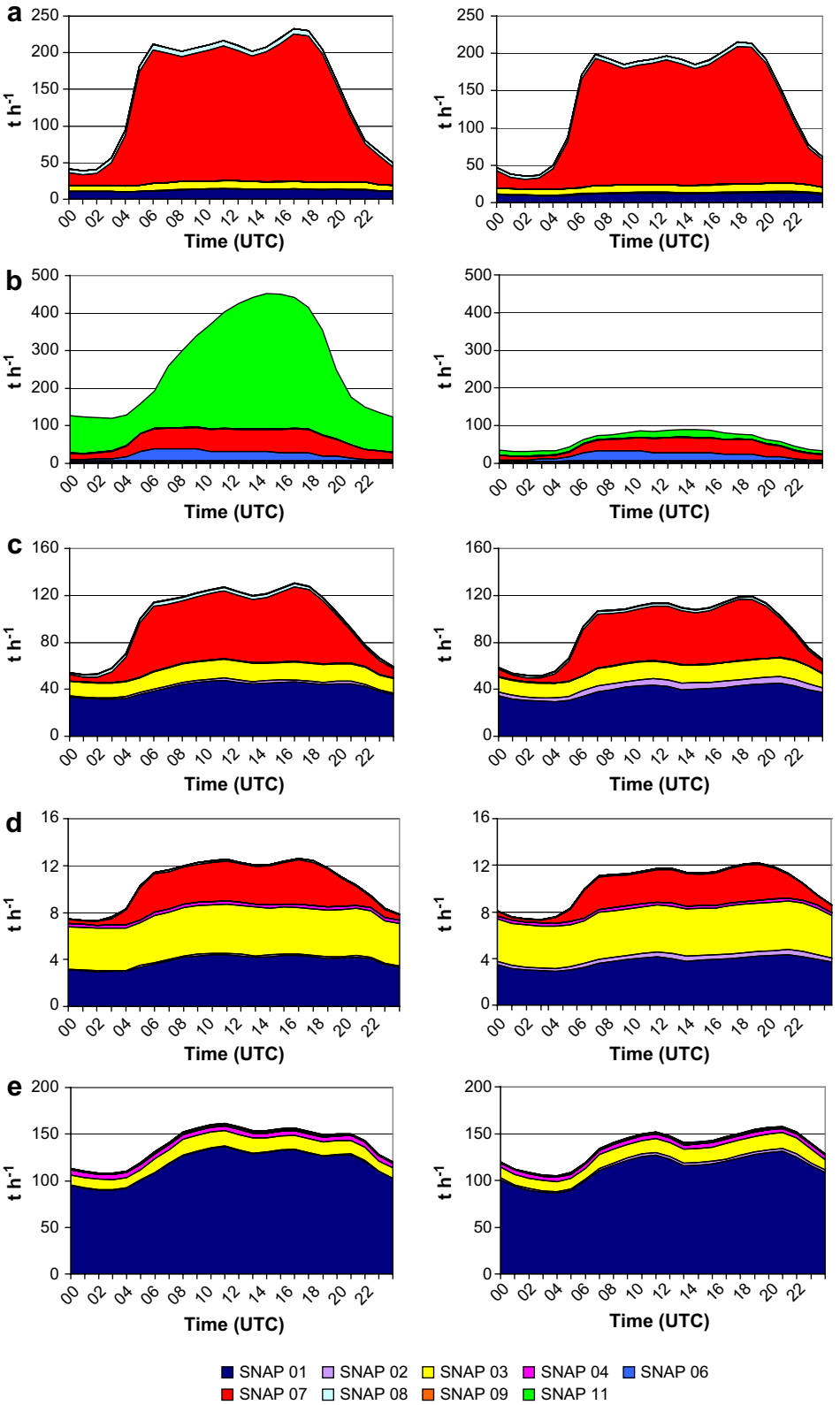

Fig. 8. Comparison of hourly variations of emissions (t h^{-1}) for one representative summer day (Monday July 26, 2004; left column) and one winter day (Monday January 19, 2004; right column) for different pollutants: (a) CO; (b) NMVOC; (c) NO_x, (d) $PM_{2.5}$; (e) SO_2.

cycles related to the weekday and weekend road traffic intensity. SO_2 emissions trend varies according to the quantity of power generated using coal, and NMVOC increases during the spring and summer presenting falls impacted by the temperature and solar radiation. The hourly emissions of NO_x, CO, SO_2 and $PM_{2.5}$ shows two peaks related with the power demand and rush hours, while NMVOC presents a curve with maximum emissions during the midday due to the high temperature and solar radiation.

Although there is a limitation in the individual sources included (biogenic emissions, power generation, the most important industrial activities, use of fossil fuels and solvents by residential and commercial sectors, road transport, ports and airports) HERMES has demonstrated its ability and accuracy for addressing emission-related problems since it has been implemented as the emission core for the validation and assessment of air quality simulations in Spain. Some future applications of the model may be related to further modelling and policy purposes for Spain. Future developments will be related to the inclusion of other sources such as urban road traffic in medium cities, paved-road resuspension, agriculture and steel industry, saltation processes, emissions from arid soils, among others.

Acknowledgments

HERMES developments were funded by the Caliope project 441/2006/3-12.1 and A357/20072-12.1 of the Spanish Ministry of the Environment.

References

van Aardenne, J.A., Dentener, F., Olivier, J.G.J., Peters, J.A.H.W., 2005. The EDGAR 3.2 Fast Track 2000 dataset (32FT2000) Emission Database for Global Atmospheric Research (http://www.mnp.nl/edgar/model/v32ft2000edgar/docv32ft2000/index.jsp#tcm:32-22076).

AEVERSU, 2005. Association for the Valorisation of Solid Municipal Wastes (http://www.aeversu.com, December 2005).

ARDAN, 2005. Information Service for the Support to the Industrial Activity. Database of Spanish Industries (http://www.ardan.es, July 2005).

Arévalo, G., Salvador, R., Gassó, S., Millán, M., Baldasano, J.M., 2004. Application of a high-resolution emission model in Valencia Community (Spain). Air Pollution 2004. WIT Press, Rhodes, Greece, pp. 31–40.

ASPAPEL, 2005. Spanish Association of Paper and Pulp Manufacturers (http://www.aspapel.es, March 2005).

Baldasano, J.M., 1998. Guidelines and formulation of an upgrade source emission model for atmospheric pollutants. In: Power, H., Baldasano, J.M. (Eds.), Air Pollution Emission Inventory. Computational Mechanics Publications. Southampton, Vol. 3. pp. 183–204.

Baldasano, J.M., Jiménez-Guerrero, P., Jorba, O., Pérez, C., López, E., Güereca, P., Martín, F., García-Vivanco, M., Palomino, I., Querol, X., Pandolfi, M., Sanz, M.J., Diéguez, J.J., 2007. Enhancing high-resolution air quality forecasting in Europe and the Iberian Peninsula within a supercomputing framework: the CALIOPE project. In: ACCENT/GLOREAM Workshop Berlin, Germany, 28–30 November 2007.

Carnevale, C., Gabusi, V., Volta, M., 2006. POEM-PM: an emission model for secondary pollution control scenarios. Environmental Modelling and Software 21, 320–329.

CEPMEIP, 2008. Coordinated European Programme on Particle Matter Emission Inventories, Projections and Guidance (available through http://www.air.sk/tno/cepmeip, May 2008).

Chang, J.P., Fontelle, J.P., Serveau, L., Allemand, N., Audoux, N., Beguier, S., Godet, E., Martinet, Y., Mathias, E., Oudart, B., Sambat, S., Vicent, J., 2007. Inventaire des Emissions de Polluants Atmospheriques en France – Series Sectorielles et Analyses Etendues. Rapport D'Inventaire National. http://www.citepa.org/publications/secten-fevrier%202007.pdf CITEPA (available through.

Colvile, R., Hutchinson, E., Mindell, J., Warren, R., 2001. The transport sector as a source of air pollution. Atmospheric Environment 35, 1537–1565.

Costa, M., Baldasano, J.M., 1996. Development of a source emission model for atmospheric pollutants in the Barcelona area. Atmospheric Environment 30A (2), 309–318.

Cros, B., Durand, P., Cachier, H., Drobinski, Ph., Fréjafon, E., Kottmeier, C., Perros, P.E., Peuch, V.-H., Ponche, J.-L., Robin, D., Saïd, F., Toupance, G., Wortham, H., 2004. The ESCOMPTE program: an overview. Atmospheric Research 68, 241–279.

Delgado, R., Toll, I., Soriano, C., Baldasano, J.M., 2000. Application to Catalonia (Spain). In: Longhurst, J.W.S., Brebbia, C., Power, H. (Eds.), Vehicle emission model of air pollutants from road traffic. Air Pollution VIII. WIT Press, pp. 379–388.

Derognat C., Beekmann M., Baeumle M., Martin D., Schmidt H., 2003. Effect of biogenic volatile organic compound emissions on tropospheric chemistry during the Atmospheric Pollution Over the Paris Area (ESQUIF) campaign in the Ile-de-France region, Journal of Geophysical Research, 108(D17), 8560.

Dore C.J., Watterson J.D., Murrells T.P., Passant N.R., Hobson M.M. Choudrie S.L., Thistlethwaite G., Wagner A., Jackson J., Li Y., Bush T., King K. R., Norris J., Coleman P.J., Walker C., Stewart R.A., Goodwin J.W.L., Tsagatakis I., Conolly C., Downes M.K., Brophy N., Hann M.R., 2007. UK Emissions of Air Pollutants 1970 to 2005 (available through http://www.naei.org.uk/reports.php).

Economopoulos, A., 1993. Assessment of Sources of Air, Water and Land Pollution. A Guide to Rapid Inventory Techniques and Use in Formulating Environmental Control Strategies. Environmental Technologies Series. World Health Organization, Geneva.

EEA, 2002. EMEP/CORINAIR Atmospheric Emissions Inventory Guidebook, third ed. October 2002 update. Technical report No 30.

EEA, 2004. European Environment Agency. EMEP/CORINAIR Emission Inventory Guidebook-2004 (available through http://reports.eea.eu.int/EMEPCORINAIR4/en/B324vs2.1.pdf).

EEA, 2007. EMEP/CORINAIR Atmospheric Emission Inventory Guidebook – 2007. Technical report 16/2007 (available through http://www.emep.int).

EMEP/CORINAIR, 2005. EMEP/CORINAIR Emission Inventory Guidebook – 2005. Snap codes, 080501–080504. Air Traffic.

François, S., Grondin, E., Fayet, S., Ponche, J.L., 2005. The establishment of the atmospheric emission inventories of the ESCOMPTE program. Atmospheric Research 74, 5–35.

Friedrich, R., Reis, S. 2004. Emission of Air Pollutants – Measurements, Calculations and Uncertainties. Genemis Eurotrac-2. Subproject Final Report. Berlin (Germany), 335 pp.

GEIA/ACCENT, 2005. GEIA-ACCENT database, an international cooperative activity of AIMES/IGBP. ACCENT EU Network of Excellence (http://www.geiacenter.org and http://www.accent-network.org).

Gery, M.W., Whitten, G.Z., Killus, J.P., Dodge, M.C., 1989. A photochemical kinetics mechanism for urban and regional scale computer modeling. Journal of Geophysical Research 94 (D10), 12925–12956.

Gómez, O., Baldasano, J.M., 1999. Biogenic VOC Emission Inventory for Catalonia, Spain. In: Borrell, P.M., Borrell, P. (Eds.), Proceedings of EUROTRAC Symposium'98. WIT Press, pp. 109–115.

Granier C., Lamarque J.F., Mieville A., Muller J.F., Olivier J., Orlando J., Peters J., Petron G., Tyndall G., Wallens S., 2005. POET, a Database of Surface Emissions of Ozone Precursors (http://www.aero.jussieu.fr/projet/ACCENT/POET.php).

Guenther, A., Hewitt, C.N., Erickson, D., Fall, R., Geron, C., Graedel, T., Harley, P., Klinger, L., Lerdau, M., McKay, W.A., Pierce, T., Scholes, B., Steinbrecher, R., Tallamraju, R., Taylor, J., Zimmerman, P., 1995. A global model of natural volatile organic compound emissions. Journal of Geophysical Research 100 (D5), 8873–8892.

Jiménez, P., Parra, R., Gassó, S., Baldasano, J.M., 2005. Modeling the ozone weekend effect in very complex terrains: a case study in the Northeastern Iberian Peninsula. Atmospheric Environment 39, 429–444.

Jiménez, P., Lelieveld, J., Baldasano, J.M., 2006. Multiscale modeling of air pollutants dynamics in the northwestern Mediterranean basin during a typical summertime episode. Journal of Geophysical Research 111, D18306, doi:10.1029/2005JD006516.

Jiménez-Guerrero, P., Jorba, O., Pérez, C., Gassó, S., Baldasano, J.M., July 2–5, 2007. Enhancing high-resolution air quality forecasting in MareNostrum Supercomputer. 11th Conference on Harmonisation within Atmospheric Dispersion Modelling for Regulatory Purposes. England, Cambridge.

Jiménez-Guerrero, P., Jorba, O., Baldasano, J.M., Gassó, S., 2008. The use of a modeling system as a tool for air quality management: annual high-resolution simulations and evaluation. Science of the Total Environment 390, 323–340.

Jorba O., Jiménez-Guerrero P., Baldasano J.M., 2008. Suitability of WRF model for air quality simulations: comparison of two dynamical cores on a yearly basis. In: European Geoscience Union (EGU) General Assembly. Vienna, April 13–18, 2008.

Kannari, A., Tonooka, Y., Baba, T., Murano, K., 2007. Development of multiple-species 1 km × 1 km resolution hourly basis emissions inventory for Japan. Atmospheric Environment 41, 3428–3439.

Lindley, S.J., Conlan, D.E., Raper, D.W., Watson, A.F.R., 2000. Uncertainties in the compilation of spatially resolved emission inventories – evidence from a comparative study. Atmospheric Environment 34, 375–388.

Meleux, F., Solmon, F., Giorgi, F., 2005. Increase in summer European ozone amounts due to climate change. Atmospheric Environment 41, 7577–7587.

Michel, C., Liousse, C., Grégoire, J.-M., Tansey, K., Carmichael, G.R., Woo, J.-H., 2005. Biomass burning emission inventory from burnt area data given by the Spot Vegetation system in the frame of TRACE-P and ACE-Asia campaigns. Journal of Geophysical Research – Atmospheres 110, D09304. doi:10.1029/2004JD005461.

Monteiro, A., Borrego, C., Miranda, A.I., Gois, V., Torres, P., Perez, A.T., 2007. Can air quality modelling improve emission inventories? In: Proceedings of the 6th International Conference on Urban Air Quality, 26–30 March, Limassol, Cyprus, pp. 13–14.

NAEI, 2007. National Atmospheric Emissions Inventory. http://www.naei.org.uk/.

Ntziachristos, L., Samaras, Z., 2000. COPERTIII Computer programme to calculate emissions from road transport. Methodology and emission factors (Version 2.1) European Environment Agency. Technical report No 49.

Ohara T., Akimoto H., Kurokawa J., Horii N., Yamaji K., Yan X., Hayasaka T., 2007. An Asian emission inventory of anthropogenic emission sources for the period 1980–2020. Atmospheric Chemistry and Physics 7, 4419–4444.

OMEL, 2005a. Mercado de la electricidad. Resultados de Mercado. Energía mensual por tecnología 2003 y 2004 (http://www.omel.es/frames/es/resultados/resultados_index.htm).

OMEL, 2005b. Mercado de la electricidad. Resultados de Mercado. Energía diaria por tecnología 2003 y 2004 (http://www.omel.es/frames/es/resultados/resultados_index.htm).

Parra, R., 2004. Desarrollo del modelo EMICAT2000 para la estimación de emisiones de contaminantes del aire en Cataluña y su uso en modelos de dispersión fotoquímica (Development of the EMICAT2000 model for the emission estimation of air pollutants and its use in photochemical dispersion models). PhD Thesis, Technical University of Catalonia (in Spanish).

Parra, R., Gassó, S., Baldasano, J.M., 2004. Estimating the biogenic emissions of non-methane volatile organic compounds from the North Western Mediterranean vegetation of Catalonia, Spain. Science of the Total Environment 329, 241–259.

Parra, R., Jimenez, P., Baldasano, J.M., 2006. Development of the high spatial resolution EMICAT2000 emission model for air pollutants from the north–eastern Iberian Peninsula (Catalonia, Spain). Environmental Pollution 140, 200–219.

Pope, C.A., Burnett, R.T., Thun, M.J., Calle, E.E., Krewski, D., Ito, K., Thurston, G.D., 2002. Lung cancer, cardiopulmonary mortality, and long-term exposure to fine particulate air pollution. Journal of the American Medical Association 287, 1132–1141.

Pulles T., Kuenen J., Pesik J., Cadman J., Wagner A., 2007. EPER Review Report 2004. European Pollutant Emission Register (EPER) (http://www.eper.ec.europa.eu).

Saamali, M., François, S., Vinuesa, J.-F., Ponche, J.-L., 2007. A new tool for processing atmospheric emission inventories: Technical aspects and application to the ESCOMPTE study area. Environmental Modelling and Software 22, 1765–1774.

Schultz, M.G., Backman, L., Balkanski, Y., Bjoerndalsaeter, S., Brand, R., Burrows, J.P., Dalsoeren, S., de Vasconcelos, M., Grodtmann, B., Hauglustaine, D.A., Mora, B., Oom, D., Pacyna, J., Panasiuk, D., Pereira, J. N.M.C., Pulles, T., Pyle, J., Rsta, S., Richter, A., Savage, N., Schnadt, C., Schulz, M., Spessa, A., Staehelin, J., Sundet, J.K., Szopa, S., Thonicke, K., van het Bolscher, M., van Noije, T., van Velthoven, P., Vik, A.F., Wittrock, F., 2007. Reanalysis of the TROpospheric Chemical Composition Over the Past 40 years (RETRO) – A Long-term Global Modeling Study of Tropospheric Chemistry. Final Report. Published Report No. 48/2007 in the Series "Reports on Earth System Science" of the Max Planck Institute for Meteorology. Hamburg. ISSN 1614-1199.

Scott Environmental Technology, 1981. Inventory of Emissions from Marine Operations Within the California Coastal Waters. Prepared for the Californian Air Resources Board by Scott Environmental Technology, Inc., San Bernardino, CA.

Streets, D.G., Bond, T.C., Carmichael, G.R., Fernandes, S.D., Fu, Q., He, D., Klimont, Z., Nelson, S.M., Tsai, N.Y., Wang, M.Q., Woo, J.H., Yarber, K.F., 2003. An inventory of gaseous and primary aerosol emissions in Asia in the year 2000. Journal of Geophysical Research 108 (D21), 8809.

Techne, 1998. Trozzi, C., Vaccaro, R.: Methodologies for Estimating Air Pollutant Emissions from Ships. Task 6.3 – Future Non-road Emissions – Ship Traffic. MEET RF98b.

TNO, 1995a. Environment, Energy and Process Innovation (TNO-MEP). Project CEPMEIP Co-ordinated European Programme on Particulate Matter Emission Inventories, Projections and Guidance. Emission factors. Production of lime [http://www.air.sk/tno/cepmeip/, October 2005].

TNO, 1995b. Environment, Energy and Process Innovation (TNO-MEP).

Tuia D., Osses de Eicker M., Zahn R., Osses M., Zarate E, Clappier A., 2007. Evaluation of a simplified top–down model for the spatial assessment of hot traffic emissions in mid-sized cities. Atmospheric Environment 41, 3658–3671.

UNFCCC, 2008. United Nations Framework Convention on Climate Change (http://unfccc.int).

Unger, N., Shindell, D.T., Koch, D.M., Streets, D.G., 2008. Air pollution radiative forcing from specific emissions sectors at 2030. Journal of Geophysical Research 113, D02306. doi:10.1029/2007JD008683.

USEPA, 1983. United States Environmental Protection Agency. Emission Factor Documentation for AP-42. Section 6.4 Organic Chemical Process Industry, May 1983.

USEPA, 1996a. United States Environmental Protection Agency. Emission Factor Documentation for AP-42. Section 3.1 Stationary Gas Turbines.

USEPA, 1996b, United States Environmental Protection Agency. Emission Factor Documentation for AP-42. Section 3.4 Large Stationary Diesel And All Stationary Dual-fuel Engines.

USEPA, 1996c. United States Environmental Protection Agency. Emission Factor Documentation for AP-42. Section 3.4 Large Stationary Diesel And All Stationary Dual-fuel Engines.

USEPA, 1996d. United States Environmental Protection Agency. Emission Factor Documentation for AP-42. Section 11.7 Ceramic Products Manufacturing, July 1996.

USEPA, 1997. United States Environmental Protection Agency. Emission Factor Documentation for AP-42. Section 11.14 Frit Manufacturing, June 1997.

USEPA, 2000. Analysis of Commercial Marine Vessels Emissions and combustible Consumption Data. Preparado por Energy and Environmental Analysis, INC.

USEPA, 2002. Emission Factor Information Emission Inventory Related Codes (http://www.epa.gov/ttn/chief/efinformation.html, February 2004).

USEPA, 2003. Air Chief 10, Emission Factor and Inventory Group. US Environmental Protection Agency. Research Triangle Park NC 27 711 CD ROM.

USEPA, 2005. Documentation for Aircraft, Commercial Marine Vessel. Locomotive and Other Non-road Components of the National Emissions Inventory Vol. I Methodology.

USEPA, 2008. National Emissions Inventory for the United States 2002 (available through http://www.epa.gov/ttn/chief/net/2002inventory.html).

Vestreng V., Breivik K., Adams K., Wagner A., Goodwin J., Rozovskaya O., Pacyna J.M., 2005. Inventory Review 2005. Emission data reported to LRTAP and NEC Directive, Initial review of HMs and POPs, EMEP/MSC-W Technical Report 1/2005, ISSN 0804–2446.

Wei, X.L., Li, Y.S., Lam, K.S., Wang, A.Y., Wang, T.J., 2007. Impact of biogenic VOC emissions on a tropical cyclone-related ozone episode in the Pearl River Delta region, China. Atmospheric Environment 41, 7851–7864.

van der Werf, G.R., Randerson, J.T., Giglio, L., Collatz, G.J., Kasibhatla, P.S., Arellano, A.F., 2006. Interannual variability in global biomass burning emissions from 1997 to 2004. Atmospheric Chemistry and Physics 6, 3423–3441.